International Immunopharmacology 67 (2019) 427–440

Contents lists available at ScienceDirect

International Immunopharmacology

journal homepage: www.elsevier.com/locate/intimp

Study of the adoptive immunotherapy on rheumatoid arthritis with Thymus-derived invariant natural killer T cells☆

Dongzhi Chen[a], Huifang Liu[a], Yuanyuan Wang[a], Shengde Chen[a], Jialin Liu[a], Wenjuan Li[a], Haiyang Dou[a], Wenguang Hou[b,**], Ming Meng[a,*]

[a] Medical School of Hebei University, Baoding, China
[b] People's Hospital of Nankai University, Tianjin, China

ARTICLE INFO

Keywords:
Rheumatoid arthritis
Cell adoptive therapy
iNKT1/iNKT2
Cytokines
Th1/Th2/Th17
Transcription factor

ABSTRACT

Background: The therapeutic effect of adoptive infusion of specific thymus-derived invariant natural killer T (iNKT) cells in a mouse model of rheumatoid arthritis (RA) was observed, and the mechanism of cellular immunotherapy was preliminarily explored.

Methods: Thymus-derived iNKT cells were infused to RA model mice, with α-GalCer as a positive control. Then, ankle swelling was examined, as well as inflammatory cell infiltration to the joint tissue (hematoxylin-eosin [H&E] staining). Flow cytometry (FCM) was used to assess iNKT cell and helper T lymphocyte (Th) subsets. Serum cytokine levels were determined with cytometric bead array (CBA), with protein expression levels of related transcription factors assessed by Western blot.

Results: The joint swelling in RA model animals were significantly improved in the cell therapy and α-GalCer positive control groups ($P < 0.05$). In addition, iNKT frequencies in peripheral blood, the thymus and spleen were increased significantly ($P < 0.05$). Meanwhile, iNKT1 subset frequencies in the thymus and spleen were decreased, as well as splenic Th1 and Th17 cell subset rates, and serum TNF-α, IFN-γ and IL-6 levels. The rates of iNKT2 and Th2 subsets as well as IL-4 and IL-10 levels were increased ($P < 0.05$). Thymus GATA-3 and splenic PLZF protein levels were increased ($P < 0.05$).

Conclusions: Adoptive infusion of thymus-derived iNKT cells exerts therapeutic effects in RA mice by increasing iNKT frequency, altering the proportions of iNKT cell subsets, correcting Th cell subset imbalance and reducing the amounts of inflammatory cytokines.

1. Introduction

RA is a complex chronic inflammatory autoimmune disease, with an incidence close to 0.5–1% [1,2]. Currently, there are no specific therapeutic drugs and methods for RA. The traditional treatment of RA mostly uses disease-modifying antirheumatic drugs (DMARDs), but it has a long cycle, significant side effects and poor patient compliance; while application of biological agents is clinically recognized for its effectiveness and importance, the associated high prices make it difficult for most patients to accept [3,4].

RA pathogenesis is mostly explained by loss of self-immune tolerance, which alters immune patterns and results in hyper-inflammatory responses. In RA, the original proliferative balance of autoreactive T cells is broken, with auxo-action for Th1 and Th17 subset hyperpolarization, releasing a large number of inflammatory cytokines. Meanwhile, the differentiation of Th2 and Treg subsets is inhibited [5,6].

In recent years, it has been found that iNKT cells play an important role as special immune regulatory cells in tumors, infections and autoimmune diseases [7,8], which are closely related to the occurrence and development of RA [9,10]. Tudhope et al. demonstrated that the majority of RA patients have iNKT cell number reduction and functional abnormalities [11]. Our previous clinical and experimental studies confirmed that the rate and in vitro proliferation of iNKT cells are significantly decreased in active RA patients compared with healthy individuals. Th1 polarization is higher in RA patients than in healthy individuals, and the rate of iNKT cells is negatively correlated with the serum IFN-γ/IL-4 ratio. The rates of iNKT cells in a mouse model of RA

☆ The authors declare no funding or conflicts of interest.

* Correspondence to: M. Meng, Medical College of Hebei University, No. 342, East Yuhua Road, Baoding 071000, China.
** Correspondence to: W. Hou, People's Hospital of Nankai University, No. 190, Jieyuan Road, Hongqiao District, Tianjin 300000, China.
E-mail addresses: 940373961@qq.com (W. Hou), mengming127@163.com (M. Meng).

https://doi.org/10.1016/j.intimp.2018.12.040
Received 27 July 2018; Received in revised form 20 November 2018; Accepted 14 December 2018
Available online 31 December 2018

are decreased, with cell dysfunction observed [12,13]. Selective adoptive infusion of iNKT cells or transgene overexpression of Vα14-Jα18 causes iNKT cells to upregulate IL-4, which can maintain immune tolerance and prevent the occurrence of autoimmune relevant type I diabetes [14]. Therefore, increasing iNKT cell rates in vivo may constitute a new strategy for RA treatment. iNKT cells are heterogeneous immuno-regulatory cells with three distinct subsets, including iNKT1 (mainly secreting IFN-γ), iNKT2 (mainly secreting IL-4), and iNKT17 (mainly secreting IL-17) [15–17]. They regulate immune responses of different types by secreting various cytokines [5,18–20], and their roles in multiple diseases may be attributed to the functions of the different subsets [20–22]. Treating different diseases with distinct iNKT cell subsets would yield better results. α-GalCer is a galactosylceramide found in marine sponge extracts, which stimulates CD1d-restricted iNKT cell activation, producing a large number of cytokines involved in immune regulation [23]. Our preliminary study obtained iNKT cells (mainly iNKT2 cell subset) from the mouse thymus. This study used α-GalCer as a positive control, and thymus-derived iNKT cells were adoptively infused into RA model mice, to assess their therapeutic effect and preliminarily explore the associated immunotherapeutic mechanism.

2. Materials and methods

2.1. Experimental animals

Sixty 6–8 week old healthy male DBA/1 mice (20.0 ± 1.5 g), reared in an SPF environment, were provided by Beijing Vital River Laboratory Animal Technology Co., Ltd. (License No. SCXK (Beijing) 2016-0006). The mice were provided drinking water and rodent chow ad libitum, and grouped after a week of adaptation. The mice were maintained under specific pathogen-free conditions in the animal facility at Animal Lab of Medical Experiment Center, Hebei University, and all experiments were approved by the Animal Welfare and Ethical Committee of Hebei University (approval number IACUC-2017009).

2.2. Reagents and instruments

The polypeptide fragments hGPI325-339 (IWYINCFGCETHAML) and hGPI469-483 (EGNRPTNSIVFTKLT) were purchased from Beijing SBS Genetech Co., Ltd. Pertussis toxin and Complete Freund's Adjuvant (CFA) were from Sigma. Eosin, hematoxylin and Tap Water/Bluing were obtained from Hibio Technology Co., Ltd. PE-T-selected-CD1d tetramer was from MBL International Woburn MA. FITC-anti-mouse TCR-β (553170), Percp-CyTM5.5 mouse anti-T-bet (561316), Alexa Fluor 647 mouse anti-PLZF (563490) and the Th1/Th2/Th17 phenotyping kit were from Becton Dickinson. Foxp3/Transcription Factor Staining Buffer was purchased from eBioscience; α-GalCer was from ENZO Life Sciences. An Olympus BX50 light microscope (Olympus) and an Accuri C6 flow cytometer (BD) were used as well.

2.3. Grouping and establishment of the mouse RA model

A total of 15 mice were randomly selected as the healthy control group, and 45 animals were subjected to artificial modeling by administration of mixed polypeptide fragments hGPI325-339 and hGPI469-483 as follows. The polypeptide fragments were mixed and dissolved in pre-cooled triple distilled water (50 μg of mixed peptide in 75 μl water), blended with the same volume of CFA to complete emulsification, then injected into the mouse tail root subcutaneously (150 μl per mouse); the same day and 48 h later, intraperitoneal injection of Pertussis toxin (200 ng each) was performed to boost immune reactions. Then, the 45 mice were randomly divided into 3 groups, including the RA model (15 mice; no treatment), α-GalCer (15 mice; subcutaneous injection of α-GalCer at 2 μg each into the tail root the day of model establishment) and cell therapy (15 mice; thymus-derived iNKT cells [mainly iNKT2 cells] at 5×10^6 by tail vein 6 days after model establishment) groups. The treatment effects were observed, and mice were sacrificed at 8, 14 and 21 days after model establishment, by cervical dislocation for sample collection.

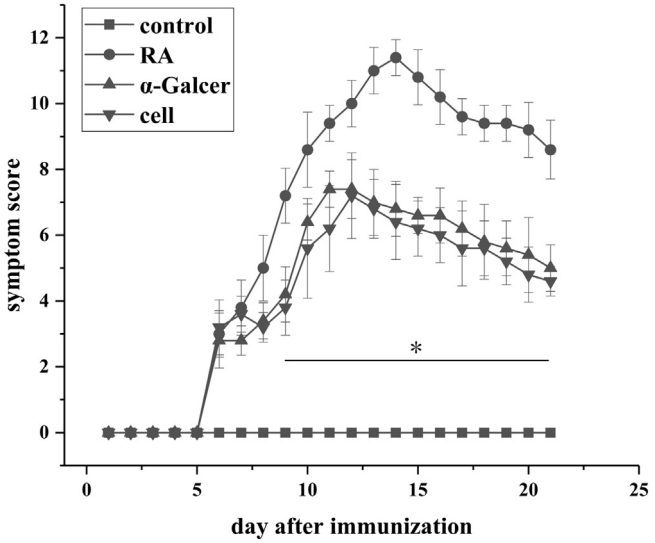

Fig. 1. Clinical score changes in different groups. *$P < 0.05$ vs RA.

2.4. General condition assessment in mice

After model establishment, ankle swelling was quantified and systematically scored daily, as follows: 1, toes with mild swelling; 2, dorsum pedis and foot pad with clearly red swelling; 3, ankle with red swelling.

2.5. Mouse joint tissue H&E staining

Blood samples were collected from the mouse eyeball at 8, 14, and 21 days after modeling, respectively. The mice were sacrificed by cervical dislocation and immersed in 75% alcohol; then, the mouse paws were excised and soaked in 10% formalin for fixation. After dehydration, the samples were paraffin embedded, sectioned (5 μm), xylene (I/II) dewaxed, hydrated with a gradient of ethanol and washed with distilled water. Hematoxylin staining was then performed for 15 min, followed by 1% ethanol eosin staining for 3 min. The sections were finally sealed and observed under a microscope.

2.6. Detection of iNKT cell rate in mouse peripheral blood

For the pre-treatment of CD1d tetramers, 1 mg/ml α-GalCer was diluted to 200 μg/ml with 0.5% Tween-20 and 0.9% NaCl, and 5 μl of the resulting solution was added to 100 μl of the CD1d tetramer solution. The mixture was incubated for 12 h at room temperature and placed at 4 °C until use. Whole blood (about 120 μl per mouse) was added to a flow-cytometry tube, followed by blocking with BSA. Then, 2 μl of each of FITC-labeled anti-CD4 and PE labeled α-GalCer-loaded CD1d tetramer were added in the dark for 20 min. Next, 1 ml of erythrocyte lytic fluid was added for 8 min away from light; after centrifugation at 1000 rpm for 5 min, the supernatant was discarded and the pellet was washed with PBS twice. Finally, the cells were resuspended in 500 μl PBS and assessed by flow cytometry (Accuri C6); the CFlow software (BD) was used for data analysis.

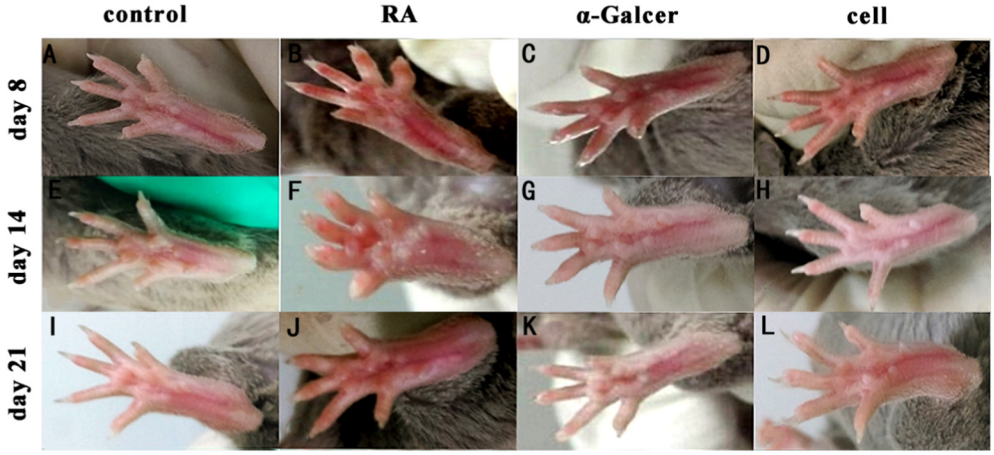

Fig. 2. Swelling of the ankle joint in mice.

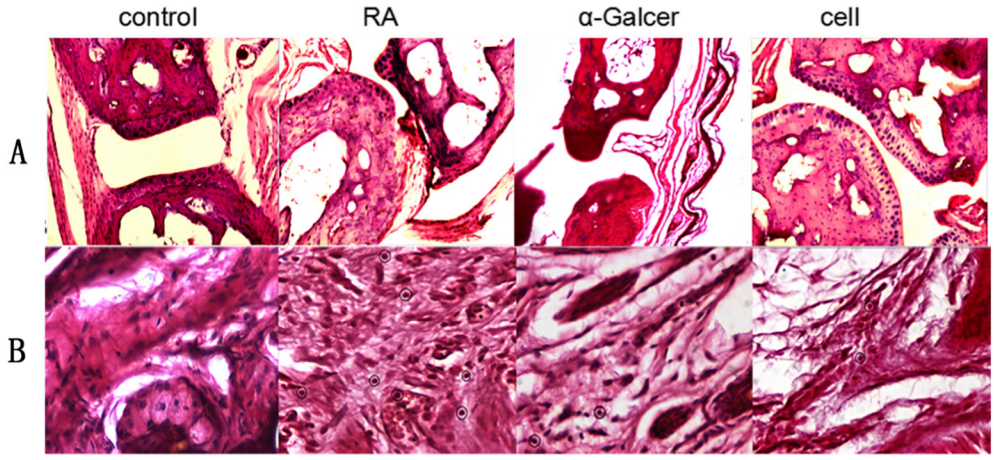

Fig. 3. Histopathological changes of the ankle joint in mice at 14 days. "○", lymphocyte; A, 100×; B, 400×.

2.7. Measurements of thymus and spleen iNKT cell rates and absolute amounts in mice

Thymocytes and spleen lymphocytes were prepared at 8, 14 and 21 days after modeling, respectively, washed twice with PBS and placed in flow cytometry tubes (1×10^6 cells/tube). Then, FITC labeled anti-TCR β (2 μl) and PE-labeled α-GalCer-loaded CD1d tetramers (2 μl) were incubated in 500 μl PBS reaction systems for 30 min in the dark, washed twice with PBS, and resuspended in 500 μl PBS for FACS detection. The absolute amounts of iNKT cells in the thymus and spleen were obtained by multiplying the total number of thymus and spleen lymphocytes by the rates of iNKT cells in lymphocytes.

2.8. Detection of iNKT cell subsets in the mouse thymus and spleen

As described in 1.7, after incubation with anti-TCR β and PE labeled α-GalCer-loaded CD1d tetramer for extracellular markers, the cells were permeabilized and fixed according to the specific procedure of Foxp3/Transcription Factor Staining Buffer. Then, 5 μl each of PerCP-Cy™ 5.5 mouse anti-T-bet and Alexa Fluor® 647 mouse anti-PLZF were added at room temperature in the dark for at least 30 min. After two washes with PBS, the cells were resuspended in 500 μl PBS and assessed by FACS.

2.9. Detection of Th1/Th2/Th17 subsets in the mouse spleen

Mouse spleen lymphocyte suspensions were prepared under aseptic conditions. The Th1/Th2/Th17 subset analysis kit was used to detect the proportions of Th1, Th2 and Th17 subsets. Cell densities were adjusted to 2×10^6/ml (culture volume was 1.5 ml), followed by addition of PMA (50 ng/ml), IO (1 μg/ml) and Monensin-containing GolgiStop (4 μl/ml). The cells were then cultured for 5 h and centrifuged at 1000 rpm for 5 min at room temperature. After washing, 10^6 cells and 1 ml of pre-cooled Cytofix solution were added to each sample, mixed and incubated in the dark at room temperature for 20 min. Next, the samples were centrifuged at room temperature and 1000 rpm for 5 min, and the cells were washed twice with PBS. After addition of 1 ml of the Perm/Wash solution at room temperature for 15 min in the dark, the cells were washed and incubated with 20 μl cocktail containing CD4-PERCP-CY5.5, IL-17A-PE, IFN-γ-FITC, and IL-4-APC diluted with 50 μl Perm/Wash, at room temperature in the dark for 30 min. After two washes with Perm/Wash, cells were resuspended in 500 μl PBS, and the Th1/Th2/Th17 subsets were detected by flow cytometry, with the CFlow software (BD) for analysis.

2.10. Cytokine contents in serum detected by CBA

Serum levels of IL-2, IL-4, IL-6, IL-10, IL-17A, IFN-γ and TNF-α were detected with the CBA cytokine kit, in strict accordance with the manufacturer's instructions. Briefly, 50 μl of each sample was assessed, and serum cytokine contents were detected on an Accuri C6 flow cytometer, using the FCAP software (BD).

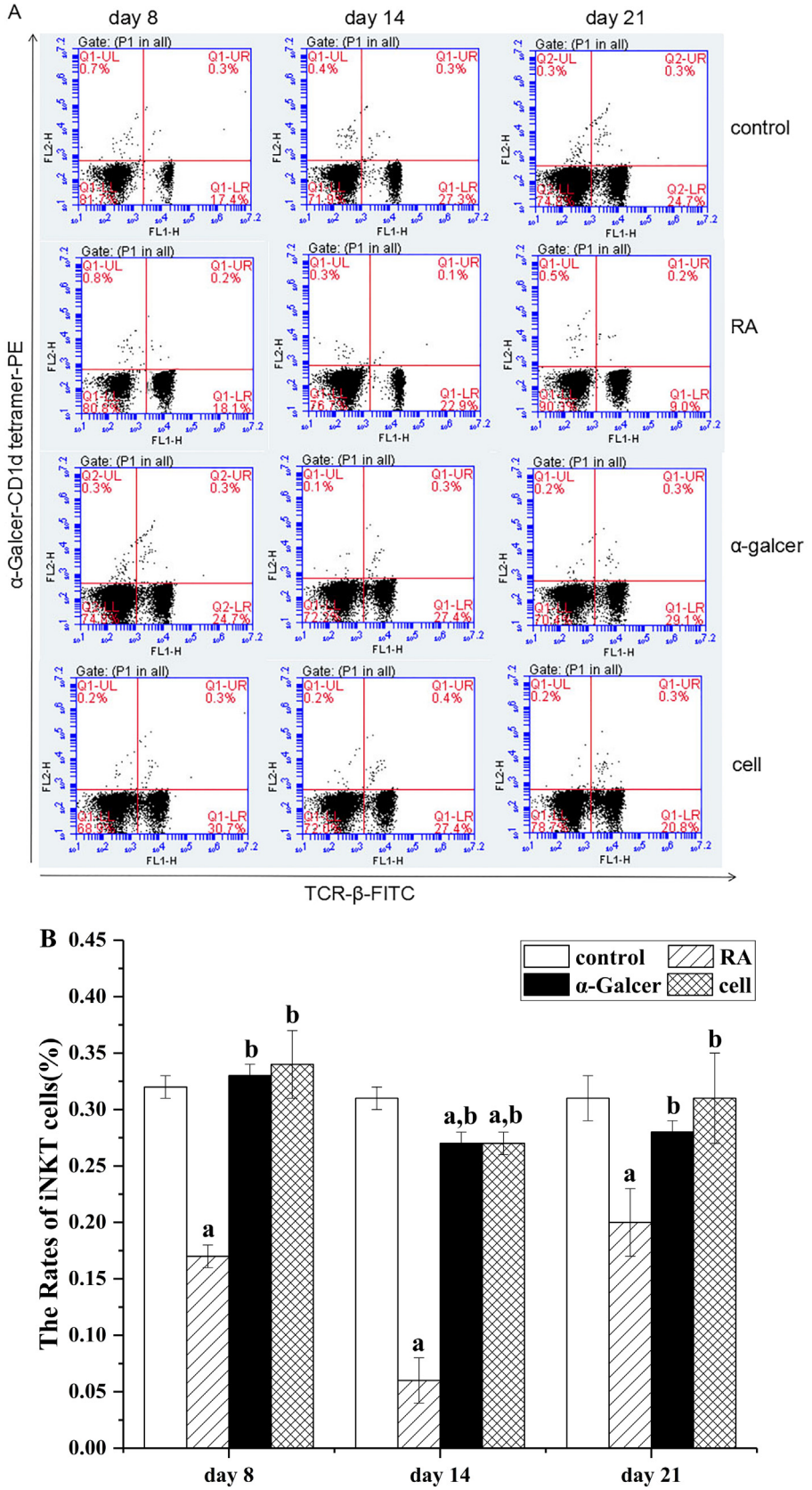

Fig. 4. Rates of iNKT cells in mouse peripheral blood. A, flow cytograms of iNKT cells in mouse peripheral blood. B, quantitation of A. $^{a}P < 0.05$ vs Control. $^{b}P < 0.05$ vs RA.

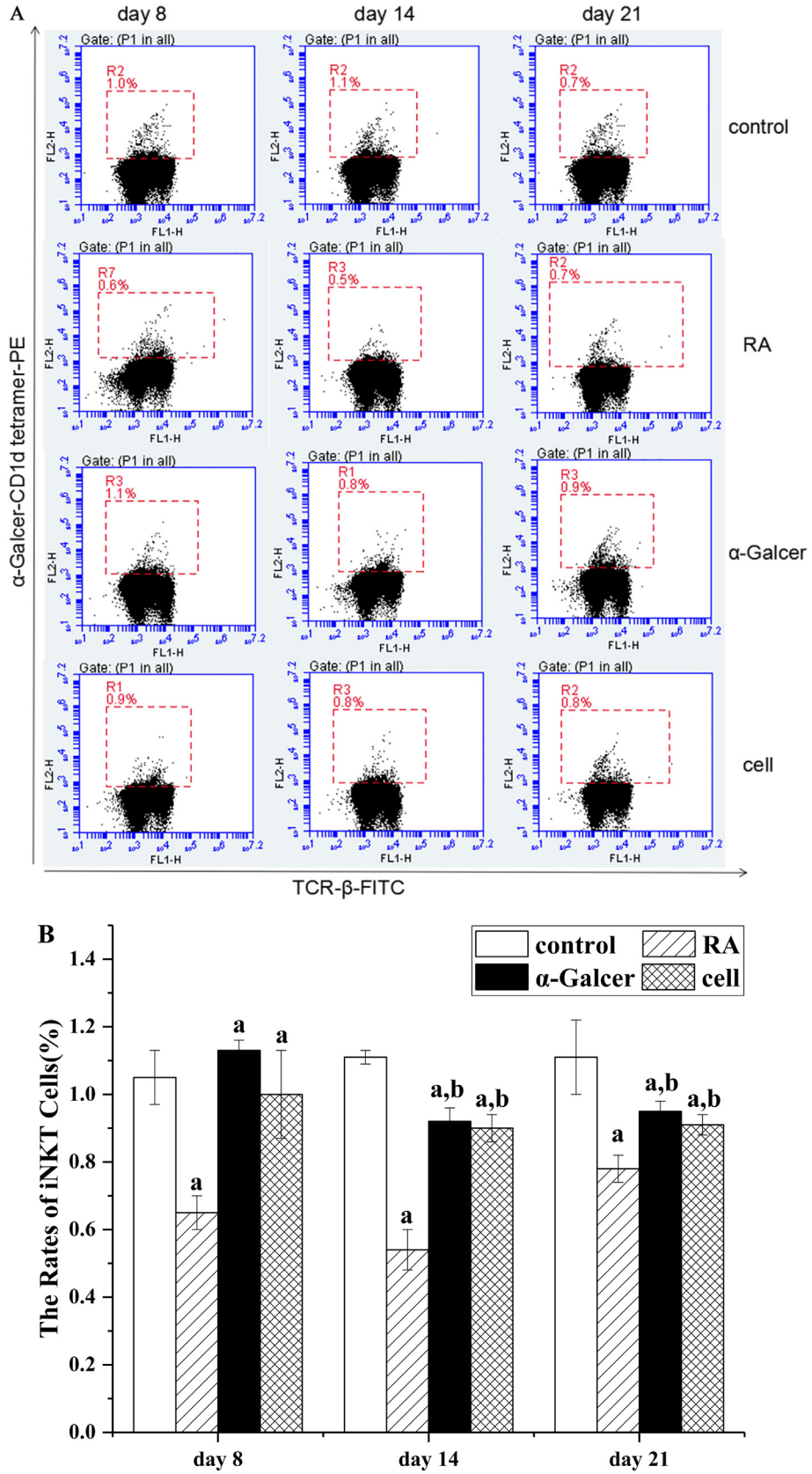

Fig. 5. Rates of iNKT cells in the mouse thymus. A, flow cytograms of iNKT in the mouse thymus. B, quantitation of A. $^{a}P < 0.05$ vs Control. $^{b}P < 0.05$ vs RA.

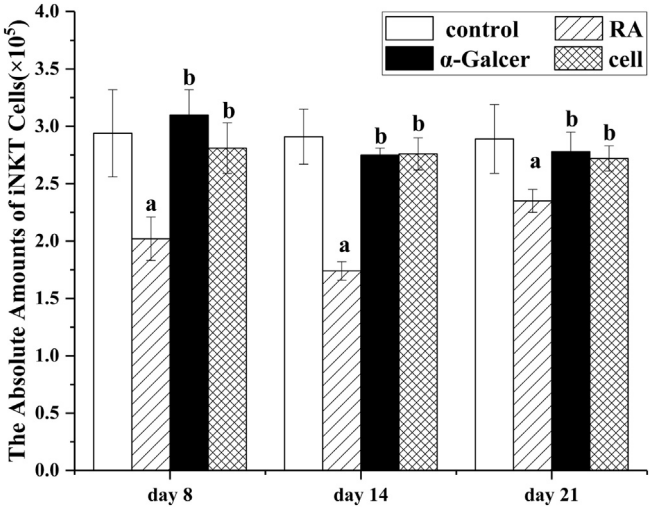

Fig. 6. Absolute amounts of iNKT cells in the mouse thymus. $^{a}P < 0.05$ vs control. $^{b}P < 0.05$ vs RA.

2.11. Quantitation of PLZF, T-Bet and GATA-3 protein levels

Thymus and spleen tissue samples (0.1 g) were used for protein extraction. Equal amounts of total protein were separated by electrophoresis and transferred onto membranes. After blocking, anti-GAPDH, anti-T-bet/Tbx21, anti-GATA3 and anti-PLZF primary antibodies (1/1000) were added for overnight incubation at 4 °C, followed by goat anti-rabbit IgG (1/1000) addition for 1 h at room temperature. The luminescent liquid was put in full contact with PVDF membranes for 2 min. Protein expression levels of PLZF in the thymus and T-bet and GATA3 in the spleen were detected by chemiluminescence. The Image J software was used to record ID values (gray scale values); GAPDH was used as an internal reference.

3. Results

3.1. Effect of iNKT cell treatment on joint swelling in RA mice

Swelling of the ankle joint in mice differed by group. In the RA model group, the toes began to show red swelling at 6 days after modeling, with gradual aggravation. At 14 days, red swelling in the ankle joint peaked, followed by gradual relief. Compared with the RA model group, the α-GalCer and cell therapy groups showed relieved swelling of the ankle joint, and ankle symptom scores were significantly decreased from 8 to 21 days ($P < 0.05$). Ankle symptom scores in the cell therapy group showed no significant difference in comparison with those of the α-GalCer group ($P > 0.05$) (Figs. 1, 2).

3.2. Effect of iNKT cell therapy on inflammatory cell infiltration in the ankle joint of RA mice

The ankle synovial tissue of RA model mice showed different degrees of inflammatory cell infiltration at various stages, with highest severity at peak inflammation (day 14). In the α-GalCer and cell therapy groups, reduced amounts of inflammatory cells were infiltrated in the synovial tissue in comparison with the RA model group (Fig. 3).

3.3. Effect of iNKT cell therapy on iNKT cell rates in peripheral blood from RA mice

Compared with the healthy control group, the model group showed significantly decreased iNKT cell rates in peripheral blood at 8, 14 and 21 days ($P < 0.05$), respectively, with the minimum at 14 days followed by a rebound at 21 days. The rates of iNKT cells in peripheral blood samples from the α-GalCer and cell therapy groups were significantly higher than those of the RA model group ($P < 0.05$). However, the rates of iNKT cells were comparable between the α-GalCer and cell therapy groups ($P > 0.05$) (Fig. 4).

3.4. Effects of iNKT cell therapy on the rate and absolute amounts of iNKT cells in the thymus of RA mice

The rate and absolute amounts of iNKT cells in the thymus of the RA model group were significantly decreased at the early (day 8), peak (day 14) and recovery (day 21) stages ($P < 0.05$) in comparison with control values. At peak inflammation, these values were minimal and rebounded in the remission phase. Compared with the RA model group, the α-GalCer and cell therapy groups showed significantly increased rates and absolute amounts of iNKT cells in the mouse thymus at all stages ($P < 0.05$). However, there were no significant differences between the α-GalCer and cell therapy groups ($P > 0.05$) (Figs. 5, 6).

3.5. Effects of iNKT cell therapy on iNKT subsets in the thymus of RA mice

Compared with healthy control animals, model mice showed significantly increased rates of the iNKT1 subset in the thymus at 8, 14, and 21 days after modeling ($P < 0.05$), respectively, peaking at 14 days. Meanwhile, the iNKT1 subset in the mouse thymus in the α-GalCer and cell therapy groups were significantly lower than those of the RA model group at all time points ($P < 0.05$), and lower in the cell therapy group compared with the α-GalCer group at the initial stages of inflammation and peak inflammation ($P < 0.05$). The frequencies of iNKT2 cells in the α-GalCer and cell therapy groups were significantly increased at the initial stage of inflammation and inflammatory remission in comparison with those of the RA model group ($P < 0.05$); the cell treatment group showed significantly higher values compared with the α-GalCer group ($P < 0.05$). Compared with control values, iNKT1/iNKT2 ratios in the RA model group were increased significantly at all stages ($P < 0.05$), reaching the maximum at peak inflammation before dropping. Compared with the RA model group, the α-GalCer and cell therapy groups showed significantly reduced iNKT1/iNKT2 ratios at all time points ($P < 0.05$). In the early stage of inflammation and peak inflammation, iNKT1/iNKT2 ratios in the cell therapy group were significantly lower than those of the α-GalCer group ($P < 0.05$) (Fig. 7).

3.6. Effects of iNKT cell therapy on the iNKT rate and absolute amounts in the spleen of RA mice

Compared with the healthy control group, the RA model group showed markedly decreased rates and absolute amounts of iNKT cells in the spleen at 8, 14, and 21 days, respectively, after modeling ($P < 0.05$), reaching the minimum at 14 days before increasing thereafter. The rates and absolute amounts of iNKT cells in the α-GalCer group were significantly increased compared with those of the RA model group at the initial stage of inflammation ($P < 0.05$); however, the cell therapy group showed no significant differences ($P > 0.05$). The rates and absolute amounts of splenic iNKT cells in the α-GalCer and cell therapy groups were significantly increased at peak inflammation ($P < 0.05$), with the cell therapy group showing significantly higher values compared with the α-GalCer group ($P < 0.05$). There were no significant differences between the two groups in the recovery phase ($P > 0.05$) (Figs. 8, 9).

3.7. Effects of iNKT cell therapy on iNKT subsets in the spleen of RA mice

In the RA model group, the rates of the iNKT1 subset in the spleen increased significantly ($P < 0.05$) at 8 and 14 days of modeling, respectively, in comparison with values of the healthy control group, peaking at 14 days, before decreasing; iNKT2 rates were significantly

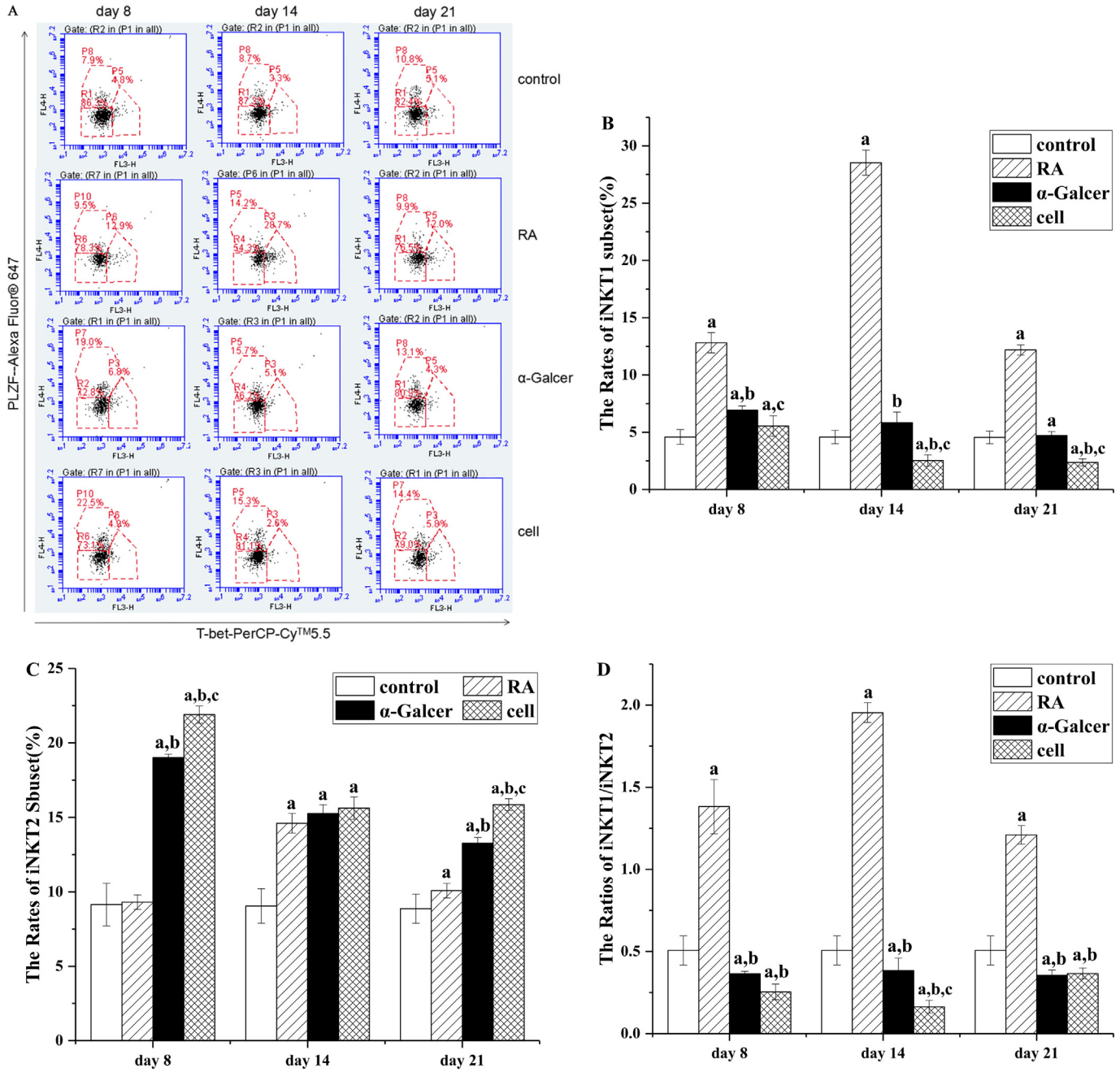

Fig. 7. Rates of iNKT1 and iNKT2 in the mouse thymus. A, flow cytograms of mouse thymus iNKT subsets. B, changes in thymic iNKT1 subsets. C, changes in thymic iNKT2 cell subsets. D, changes of the iNKT1/iNKT2 ratio in the mouse thymus. $^{a}P < 0.05$ vs Control. $^{b}P < 0.05$ vs RA. $^{c}P < 0.05$ vs α-GalCer.

increased at 21 days after modeling ($P < 0.05$); iNKT1/iNKT2 ratios were significantly higher at the initial and peak stages ($P < 0.05$), peaked, and then decreased. Compared with the RA model group, the α-GalCer and cell treatment groups showed significantly decreased rates of iNKT1 cells in the spleen at peak inflammation ($P < 0.05$); in addition, iNKT2 rates in the spleen of the α-GalCer and cell therapy groups at the early stage of inflammation and inflammatory remission were significantly increased ($P < 0.05$), with the cell therapy group showing significantly higher values compared with the α-GalCer group ($P < 0.05$); iNKT1/iNKT2 ratios in the α-GalCer and cell therapy groups were significantly lower at the initial stage of inflammation and peak inflammation, respectively ($P < 0.05$). The cell therapy group showed significantly lower iNKT1/iNKT2 ratios compared with the α-GalCer group ($P < 0.05$) (Fig. 10).

3.8. Effects of iNKT cell therapy on helper T cell (Th) subsets in the spleen of RA mice

Compared with the healthy control group, the RA model group showed significantly increased Th1 and Th17 subset rates at the early stage of inflammation, while the Th2 subset had no change. At peak inflammation and during remission, the proportions of Th1 and Th17 subsets were decreased, while the Th2 subset was increased significantly ($P < 0.05$). The proportion of the Th2 subset was significantly increased at the initial stage of inflammation in the cell treatment and α-GalCer groups in comparison with the RA model group; the change in cell therapy group was more obvious ($P < 0.05$) (Fig. 11).

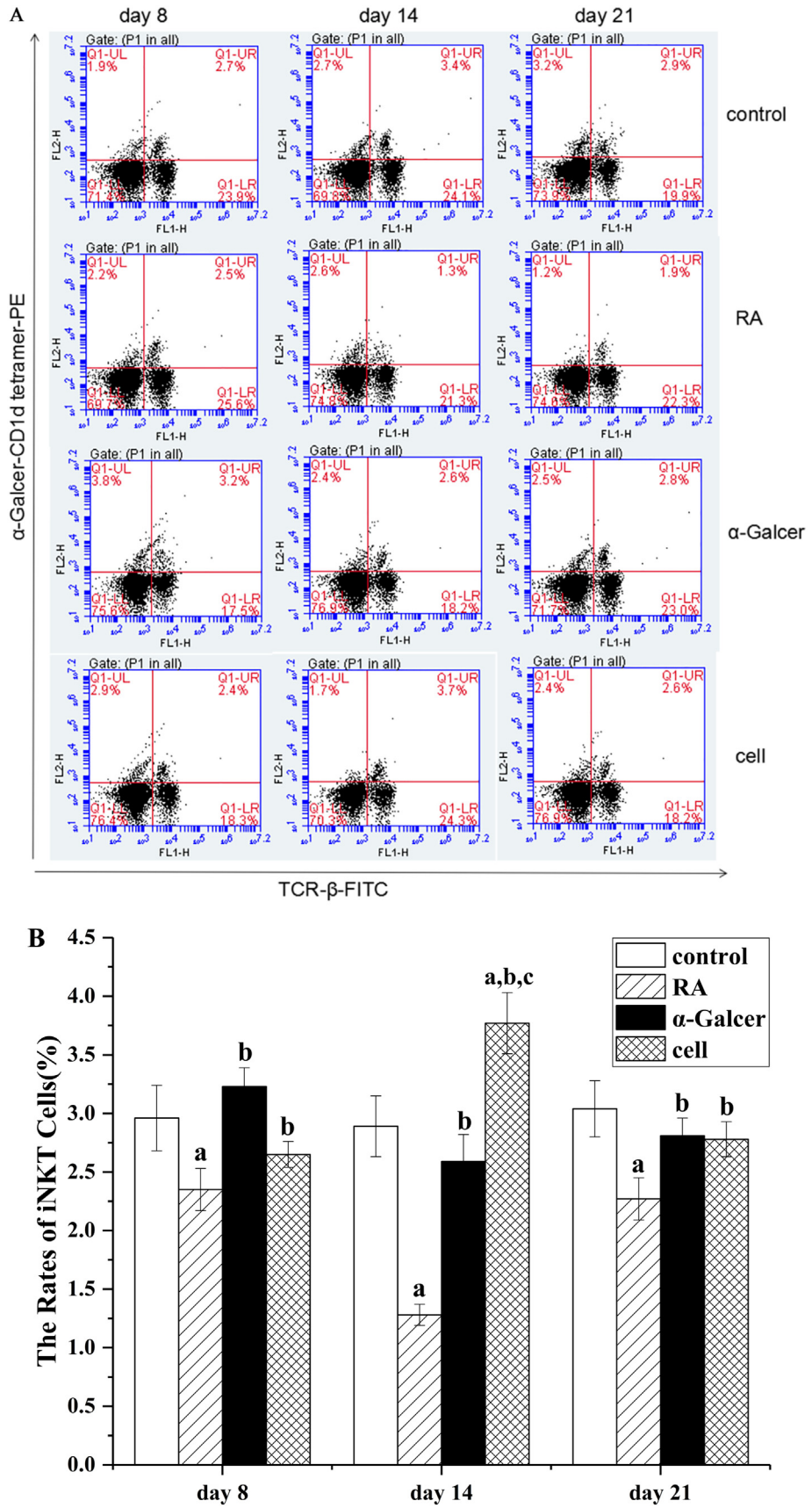

Fig. 8. Rates of iNKT cells in the mouse spleen. A, Flow cytograms of iNKT cells in the mouse spleen; B, quantitation of A. $^{a}P < 0.05$ vs Control. $^{b}P < 0.05$ vs RA. $^{c}P < 0.05$ vs α-GalCer.

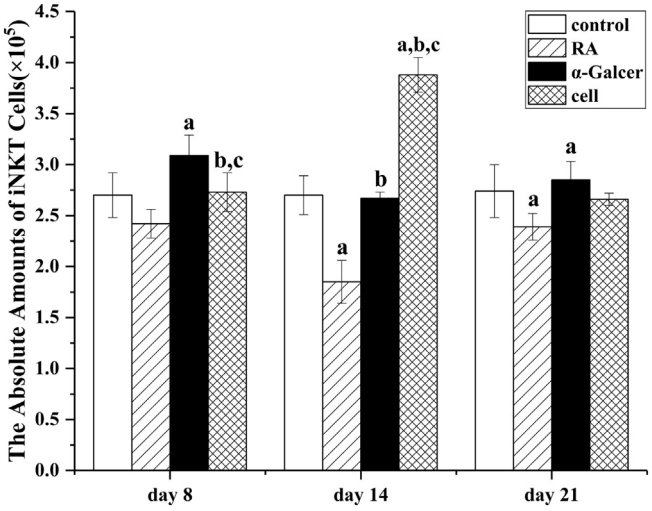

Fig. 9. Absolute amounts of iNKT cells in the mouse spleen. $^{a}P < 0.05$ vs control. $^{b}P < 0.05$ vs RA. $^{c}P < 0.05$ vs α-GalCer.

3.9. Effects of iNKT cell therapy on serum cytokine levels

The serum levels of inflammatory cytokines (TNF-α, IFN-γ and IL-6) in the RA model group were significantly increased in comparison with control values ($P < 0.05$), while anti-inflammatory cytokines (IL-4 and IL-10) showed markedly decreased amounts ($P < 0.05$). Compared with the RA model group, the α-GalCer and iNKT cell therapy groups showed significantly decreased serum levels of inflammatory cytokines (TNF-α, IFN-γ and IL-6) at the early stage of inflammation as well as peak inflammation ($P < 0.05$), while anti-inflammatory cytokines (IL-4 and IL-10) showed significantly increased levels ($P < 0.05$) (Tables 1, 2).

3.10. Effects of iNKT cell therapy on the expression of key proteins in the thymus and spleen

We assessed the protein expression levels in the healthy control and RA model groups, and found that at the initial stage of inflammation, the PLZF protein in the thymus of RA model mice was significantly downregulated ($P < 0.05$), while the T-bet protein in the spleen was significantly upregulated ($P < 0.05$); the GATA3 protein showed no significant difference. At peak inflammation, there was no significant difference in PLZF protein expression in the thymus of RA model mice ($P > 0.05$), while spleen T-bet amounts remained elevated ($P < 0.05$), and GATA3 protein levels were significantly increased ($P < 0.05$). Compared with the RA model group, the α-GalCer and iNKT cell therapy groups had significantly increased thymic PLZF protein expression levels at the initial and peak stages of inflammation ($P < 0.05$). Splenic T-bet protein amounts showed no significant difference ($P > 0.05$), but GATA3 protein levels were significantly increased in the initial inflammatory stage ($P < 0.05$); meanwhile, GATA3 protein amounts were significantly decreased at peak inflammation ($P < 0.05$) in the α-GalCer group, with no significant difference in the iNKT cell infusion group ($P > 0.05$) (Figs. 12, 13).

4. Discussion

iNKT cells are critical for immune regulation [24], controlling the functions and differentiation of other immune cells by releasing cytokines and via direct contact [25]. Studies have shown that iNKT cells can secrete IFN-γ to promote Th0 cell differentiation into Th1 cells, and secrete IL-4 to promote Th0 cell differentiation into Th2 cells [26], playing a key role in correcting the Th1/Th2 balance and inhibiting excessive inflammation [27,28].

Activation of iNKT cells as a new RA bio-therapeutic tool has attracted considerable attention. Masanobu Horikoshi et al. [29] significantly inhibited GPI peptide-induced arthritis by suppressing CD4 + T by intradermal injection of α-GalCer. Chiba et al. [30] showed that repeated injections of the synthetic α-GalCer analogue OCH (an iNKT2 selective activator) inhibit the clinical and pathological processes of CIA, while injection of α-GalCer showed slight inhibition. A preliminary study of single subcutaneous injection of α-GalCer into the tail root found that the rate of the thymic iNKT1 subset in mice reached the minimum (about 0.31%) while that of the iNKT2 subset peaked (about 50%) at 8 days. Purified thymic iNKT cells by MACS could achieve a purity of about 70%, and these cells mainly secrete IL-4. Adoptive infusion of thymus-derived iNKT cells into RA model mice resulted in significantly improved ankle swelling, reduced inflammatory cell infiltration to the joint tissue, increased serum IL-4 and IL-10 levels and reduced serum IFN-γ and TNF-α amounts. It was shown that adoptive treatment with thymus-derived iNKT cells possessing specific phenotypes and functions has the same efficacy as α-GalCer administration, which inhibits excessive inflammatory reactions in RA mice and effectively relieves RA progression. We found that the rates and absolute amounts of iNKT cells in peripheral blood, the thymus and spleen were significantly lower in the RA model group compared with the healthy control group at all time points, consistent with previous reports [31,32]; meanwhile, the cell therapy and α-GalCer (positive control) groups showed significantly increased values in comparison with the RA model group. At the inflammatory peak stage, the rate of splenic iNKT cells was more pronouncedly increased in the cell therapy group than in the α-GalCer group. Few reports have assessed changes in iNKT subsets during the pathogenesis of RA. Further detection of iNKT cell subsets in the thymus and spleen showed that the proportions of the iNKT1 subset in the RA model group were significantly increased than control values at the initial, peak and recovery stages of inflammation, with most obvious changes at peak inflammation. However, the iNKT2 subset frequency did not increase until peak inflammation. These findings suggested that the iNKT1 subgroup may be involved in early inflammation in RA, while the iNKT2 subgroup likely has important functions in inhibiting inflammation. Compared with the RA model group, the α-GalCer and cell therapy groups showed significantly decreased iNKT1 subset rates in the thymus and spleen in the inflammatory phase, with cell therapy being superior to α-GalCer administration in terms of efficacy. The iNKT2 subset was significantly increased in the early and recovery stages of inflammation, and the cell-therapy group showed more pronouncedly increased frequency compared with the α-GalCer group. These results demonstrate that adoptive infusion of iNKT cells with specific phenotypes and functions significantly increases the rates of iNKT cells and alters the proportions of iNKT cell subsets in RA. It is worth noting that we previously observed iNKT cell distribution after adoptive infusion in mice by the in vivo small animal imaging technique, and found that the infused cells mainly reside in the liver and spleen, and not found in the thymus. Therefore, we hypothesize that these cells may regulate the development and differentiation of iNKT cells via the cytokine pathway in the thymus after adoptive infusion, which deserves further investigation.

An important pathological mechanism of RA pathogenesis is excessive polarization of Th1 and Th17 subsets leading to the release of a large number of inflammatory cytokines, with reduced differentiation of Th2 and Treg subsets [5,6]. To determine whether adoptive infusion of iNKT cells with specific phenotypes and functions can inhibit excessive inflammatory responses in rheumatoid arthritis by correcting the imbalance of helper T cell (Th) subsets, Th1, Th2, and Th17 subsets in the spleen were assessed. The results showed that Th1 and Th17 subsets were increased significantly at the early stage of inflammation in RA models, while the Th2 subset was markedly increased at peak inflammation, compared with healthy controls. Compared with the RA model group, the cell therapy and α-GalCer groups showed significantly increased Th2 subset frequencies at the early stage of inflammation,

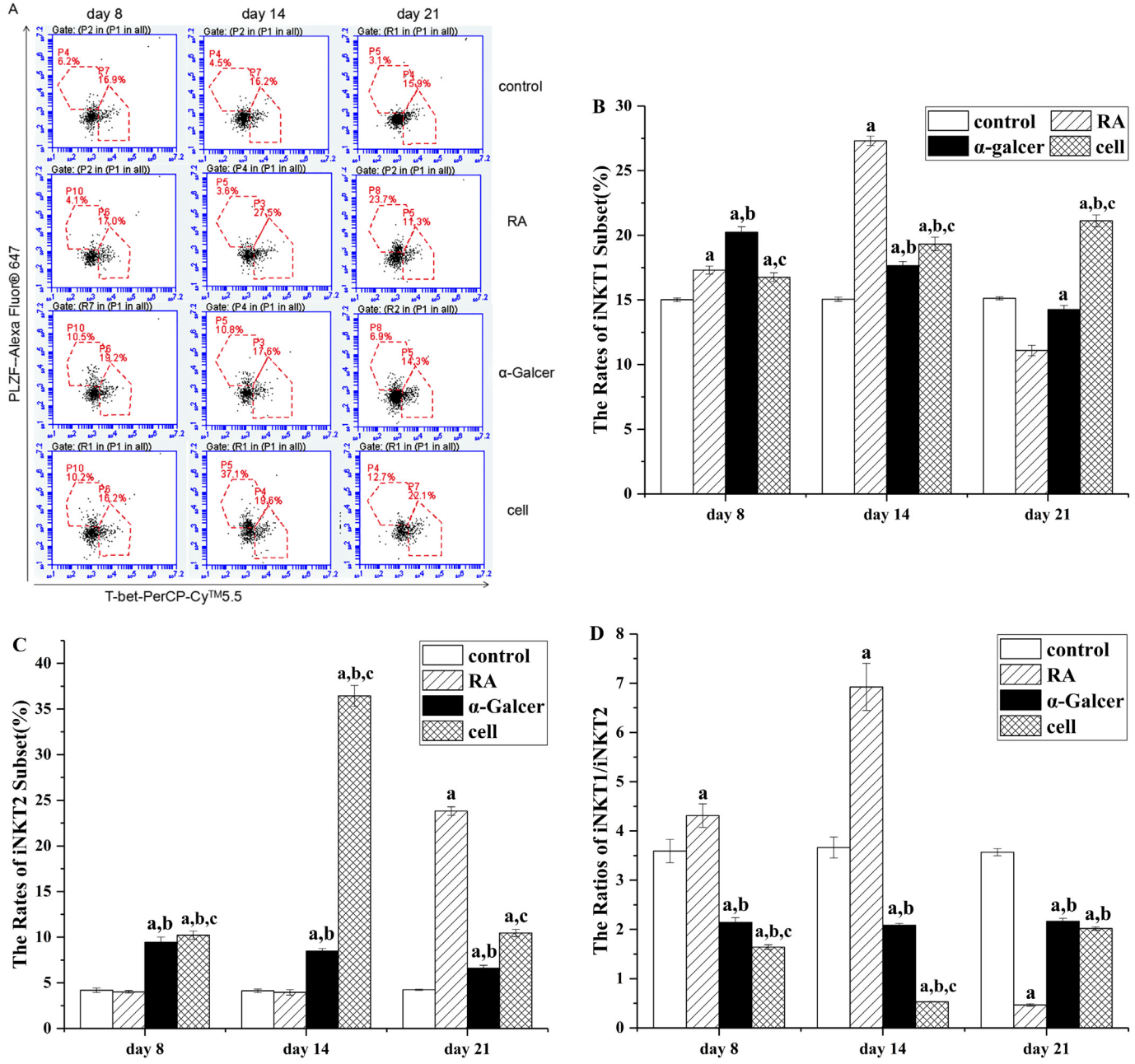

Fig. 10. Rates of iNKT1 and iNKT2 cells in the mouse spleen. A, flow cytograms of iNKT subpopulations in the mouse spleen. B, changes in iNKT1 subpopulations. C, changes in iNKT2 cell subsets. D, changes of iNKT1/iNKT2 ratios. $^{a}P < 0.05$ vs Control. $^{b}P < 0.05$ vs RA. $^{c}P < 0.05$ vs α-GalCer.

with cell therapy being superior to α-GalCer administration. These findings suggested that adoptive infusion of iNKT cells could inhibit excessive inflammation; this may reverse the immune imbalance caused by increased Th1 and Th17 subsets, which are more pronounced at the early stage of RA inflammation. Therefore, early inflammation in RA is likely the best period for cell therapy.

PLZF is an essential transcription factor in the development of iNKT cells. Increased protein expression of PLZF indirectly reflects iNKT development in the mouse thymus [33–37]. Western blot analysis of relevant transcription factors in the thymus and spleen showed that thymus PLZF expression in the RA model group at the early stage of inflammation was significantly decreased compared with the control value, indicating defective development of iNKT cells in the thymus of RA mice. Adoptive infusion of iNKT cells significantly increased the protein levels of PLZF in the thymus of RA model mice, further validating the above cell-level assay data. Compared with healthy control mice, the RA model group showed significantly increased splenic T-bet expression at the initial and peak stages of inflammation, while GATA3 was significantly upregulated at peak inflammation. GATA3 expression levels in the cell therapy group were significantly increased at the early stage of inflammation in the mouse spleen. This suggests that adoptive infusion of iNKT cells into mice may upregulate GATA3 in Th cells and promote Th0 differentiation into Th2 cells, thereby inhibiting inflammatory responses.

In summary, adoptive infusion of iNKT cells with specific phenotypes and functions can modulate thymic iNKT cell development, restore iNKT cell frequency in RA mice, modulate the iNKT1/iNKT2 cell ratio and correct the Th (Th1/Th2) cell subset imbalance, inhibiting excessive inflammatory responses, with a positive effect on RA relief.

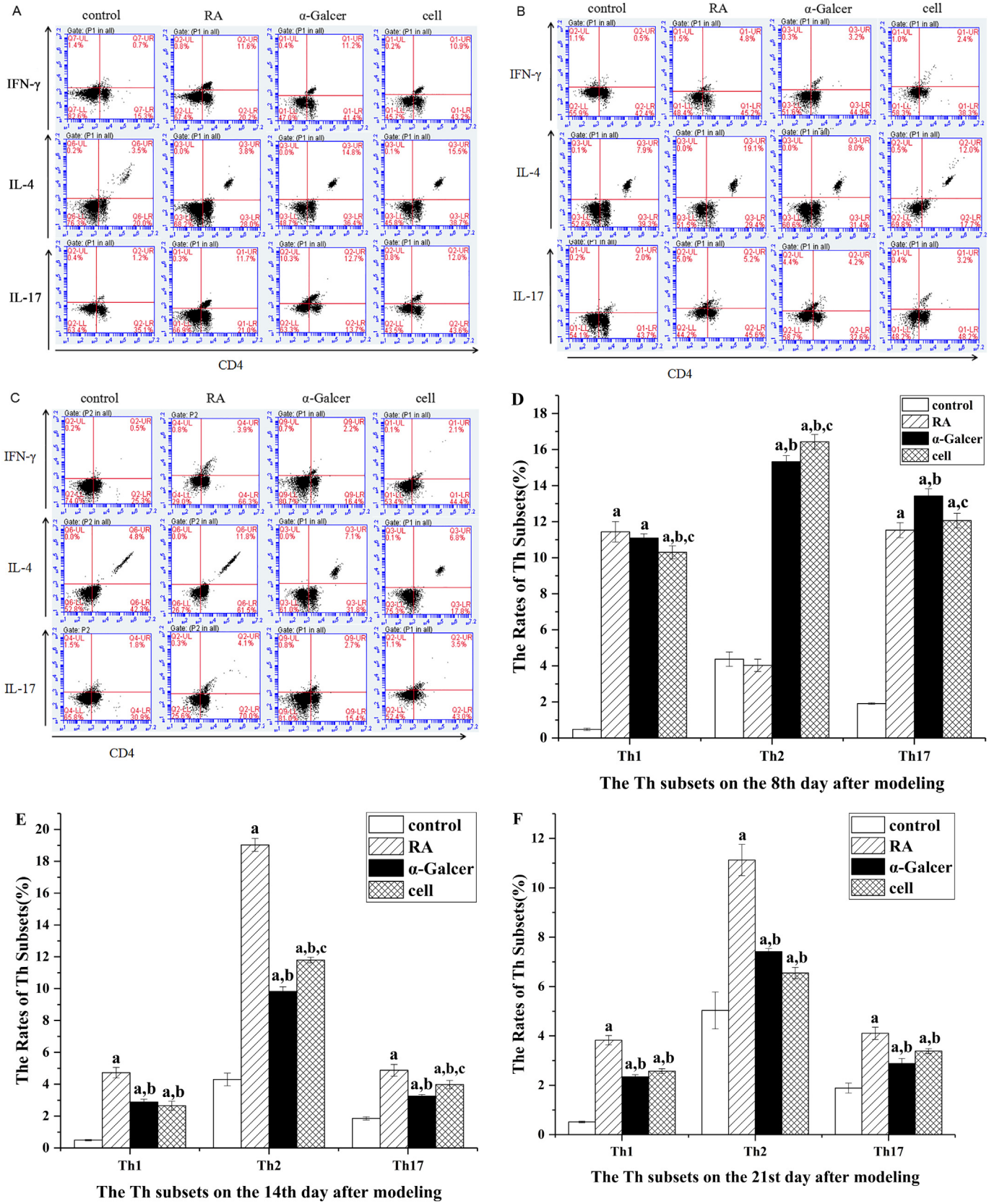

Fig. 11. Rates of Th subsets in the mouse spleen. A, B and C, flow cytograms of spleen Th subsets at 8, 14 and 21 days after modeling. D, E and F are quantitative data of A, B and C, respectively. [a]$P < 0.05$ vs Control. [b]$P < 0.05$ vs RA. [c]$P < 0.05$ vs α-GalCer.

Table 1
Serum cytokine levels in mice at 8th day after modeling (pg/ml).

Cytokines		Control	RA	α-GalCer	Cell
Proinflammatory cytokine	TNF-α	2.77 ± 0.24	10.66 ± 0.96[a]	6.9 ± 0.42[a,b]	4.44 ± 0.21[a,b]
	IFN-γ	0.26 ± 0.03	3.02 ± 0.13[a]	1.10 ± 0.15[a,b]	1.09 ± 0.02[a,b]
	IL-2	1.31 ± 0.09	1.26 ± 0.06	1.37 ± 0.08	1.25 ± 0.03
	IL-6	25.62 ± 0.17	36.83 ± 0.40[a]	28.33 ± 0.40[a,b]	26.12 ± 0.57[b]
	IL-17A	Below detection			
Anti-inflammatory cytokine	IL-4	2.21 ± 0.11	1.95 ± 0.20	2.63 ± 0.36[a,b]	2.94 ± 0.30[a,b]
	IL-10	4.32 ± 0.31	1.23 ± 0.21[a]	3.15. ± 0.33[a,b]	4.31 ± 0.06[a,b]

n = 5.
[a] $P < 0.05$ vs Control.
[b] $P < 0.05$ vs RA.

Table 2
Serum cytokine levels in mice at 14th day after modeling (pg/ml).

Cytokines		Control	RA	α-GalCer	Cell
Proinflammatory cytokine	TNF-α	2.77 ± 0.24	17.23 ± 0.26[a]	8.07 ± 0.30[a,b]	8.20 ± 0.34[a,b]
	IFN-γ	0.26 ± 0.03	7.47 ± 0.21[a,b]	1.14 ± 0.12[a,b]	0.38 ± 0.02[b]
	IL-2	1.31 ± 0.09	1.25 ± 0.09	1.31 ± 0.04	1.23 ± 0.03
	IL-6	25.62 ± 0.17	50.74 ± 1.25[a]	25.20 ± 1.03[a,b]	25.81 ± 0.42[b]
	IL-17A	Below detection			
Anti-inflammatory cytokine	IL-4	2.21 ± 0.11	1.52 ± 0.09[a]	2.56 ± 0.38[b]	2.69 ± 0.34[b]
	IL-10	4.32 ± 0.31	1.39 ± 0.04[a]	4.59 ± 0.35[b]	4.54 ± 0.07[b]

n = 5.
[a] $P < 0.05$ vs Control.
[b] $P < 0.05$ vs RA.

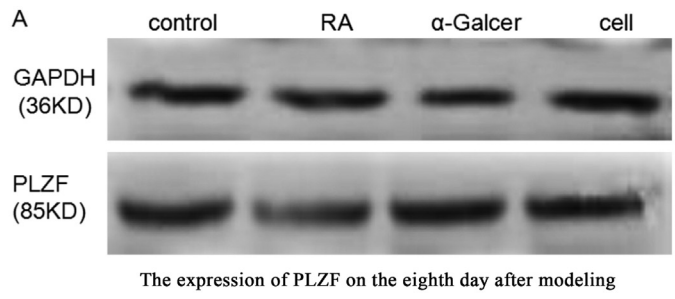

The expression of PLZF on the eighth day after modeling

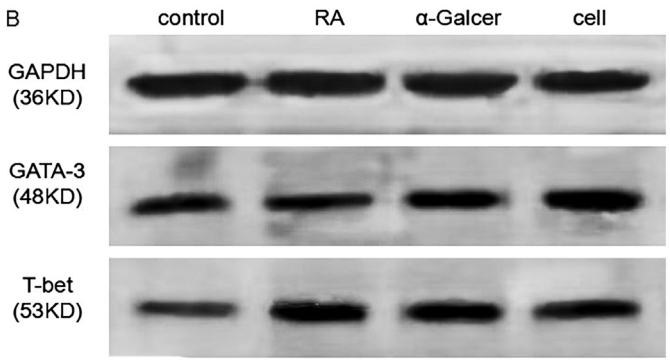

The expression of GATA3 and T-bet on the eighth day after modeling

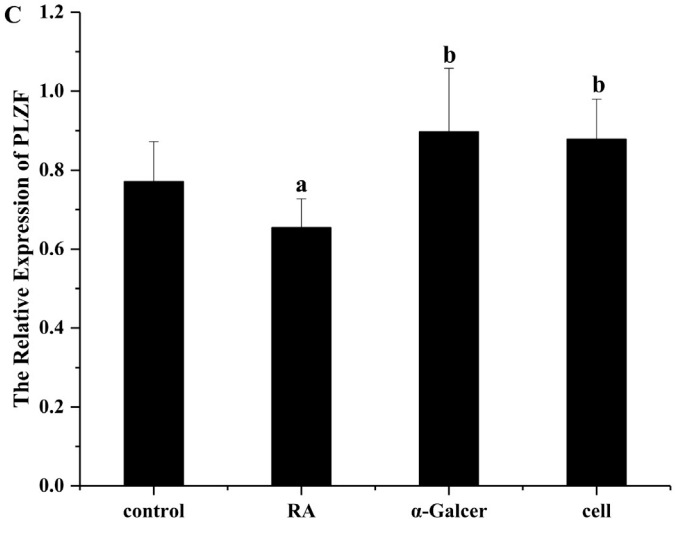

The expression of PLZF on the 8th day after modeling

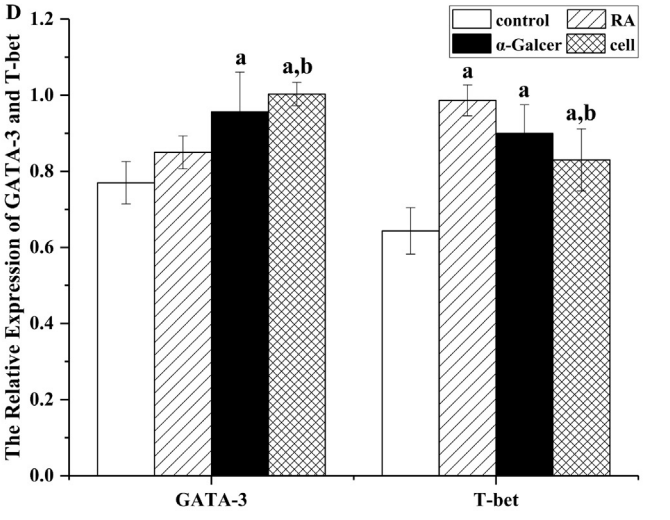

The expression of GATA-3 and T-bet on the 8th day after modeling

Fig. 12. Relative expression levels of various proteins in the thymus and spleen of mice at 8 days. A and C, relative expression of PLZF in the thymus. B and D, relative amounts of T-bet and GATA-3 in the spleen. [a]$P < 0.05$ vs control. [b]$P < 0.05$ vs RA.

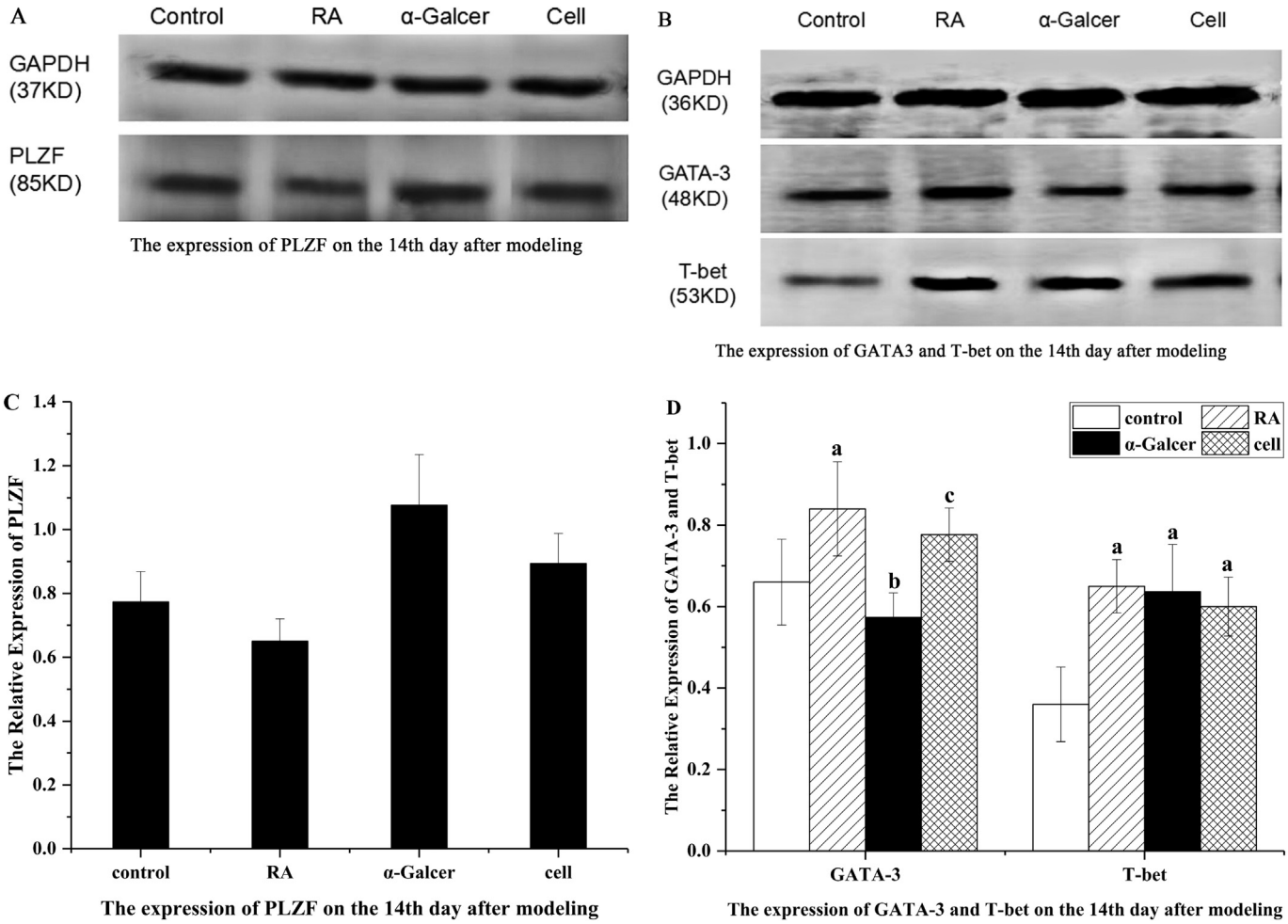

Fig. 13. Relative expression levels of various proteins in the thymus and spleen of mice at 14 days. A and C, relative expression of PLZF in the thymus. B and D, relative amounts of T-bet and GATA3 in the spleen. $^{a}P < 0.05$ vs control. $^{b}P < 0.05$ vs RA. $^{c}P < 0.05$ vs α-GalCer.

Acknowledgements

We are grateful to the National Natural Science Foundation of China (NSFC) (81771755), the Natural Science Foundation of Hebei Province (H2015201131), Colleges and university's Science and Technology Key Research Project of Hebei Province (ZD2017009), the Graduate Innovation Funding Project of Hebei University(x201740), the Undergraduate Innovation and Entrepreneurship Training Program (201710075017) and the Animal Lab of Medical Experiment Center, Hebei University for their support.

References

[1] G.J. Tobon, P. Youinou, A. Saraux, The environment, geo-epidemiology, and autoimmune disease: rheumatoid arthritis, J. Autoimmun. 35 (2010) 10–14.
[2] M. Cross, E. Smith, D. Hoy, L. Carmona, F. Wolfe, T. Vos, B. Williams, S. Gabriel, M. Lassere, N. Johns, R. Buchbinder, A. Woolf, L. March, The global burden of rheumatoid arthritis: estimates from the global burden of disease 2010 study, Ann. Rheum. Dis. 73 (2014) 1316–1322.
[3] J.A. Singh, K.G. Saag, S.L. Bridges Jr.et al., American College of Rheumatology guideline for the treatment of rheumatoid arthritis, Arthritis Care Res. 68 (1) (2015) 1–25 2016.
[4] J.S. Smolen, R. Landewe, F.C. Breedveld, et al., EULAR recommendations for the management of rheumatoid arthritis with synthetic and biological disease-modifying antirheumatic drugs: 2013 update, Ann. Rheum. Dis. 73 (3) (2014) 492–509.
[5] G. Vahedi, Y. Kanno, Y. Furumoto, et al., Super-enhancers delineate disease-associated regulatory nodes in T cells, Nature 520 (2015) 558–562.
[6] M.C. Boissier, E. Assier, G. Falgarone, et al., Shifting the imbalance from Th1/Th2 to Th17/Treg: the changing rheumatoid arthritis paradigm, Joint Bone Spine 75 (2008) 373–375.
[7] A. Torina, G. Guggino, M.P. La Manna, et al., The Janus face of NKT cell function in autoimmunity and infectious diseases, Int. J. Mol. Sci. 19 (2) (2018) 440.
[8] M. Bedard, M. Salio, V. Cerundolo, Harnessing the power of iNKT cells in cancer immunotherapy, Front. Immunol. 8 (2017) 1829.
[9] P.J. Brennan, M. Brigl, M.B. Brenner, Invariant natural killer T cells: an innate activation scheme linked to divers, Nat. Rev. Immunol. 13 (2) (2013) 101–117.
[10] M. Gol-Ara, F. Jadidi-Niaragh, R. Sadria, et al., The role of different subsets of regulatory T cells in immunopathogenesis of rheumatoid arthritis, Arthritis 2012 (2012).
[11] S.J. Tudhope, A. von Delwig, J. Falconer, et al., Profound invariant natural killer T-cell deficiency in inflammatory arthritis, Ann. Rheum. Dis. 69 (10) (2010) 1873–1879.
[12] Meng Ming, Chen Dan, Xu Minghua, et al., Study of the correlation between the percentage of iNKT cells and the ratio of IFN-γ/IL-4 in patients with rheumatoid arthritis, Chin. J. Microbiol. Immunol. 35 (3) (2015) 213–218.
[13] Xue-jiao Zhang, Jia-lin Liu, Fei Yang, et al., Immunization with mixed peptides derived from glucose-6-phosphate isomerase induces rheumatoid arthritis in DBA/1 mice, Chin. J. Pathophysiol. 32 (3) (2016) 569–576.
[14] S. Sharif, G.A. Arreaza, P. Zucker, et al., Activation of natural killer T cells by α-galactosylceramide treatment prevents the onset and recurrence of autoimmune Type 1 diabetes, Nat. Med. 7 (2010) 1057–1062.
[15] L. Gapin, Development of invariant natural killer T cells, Curr. Opin. Immunol. 39 (2016) 68–74.
[16] D. Kwon, Y.J. Lee, Lineage differentiation program of invariant natural killer T cells, Immune Netw. 17 (6) (2017) 365–377.
[17] P. Thapa, B. Manso, J.Y. Chung, et al., The differentiation of ROR-γt expressing iNKT17 cells is orchestrated by Runx1, Sci. Rep. 7 (1) (2017) 7018.
[18] C.W. Keller, S. Freigang, J.D. Lünemann, Reciprocal crosstalk between dendritic cells and natural killer T cells: mechanisms and therapeutic potential, Front. Immunol. 8 (2017) 570.
[19] F.A. Ververs, E. Kalkhoven, B. Van't Land, et al., Immunometabolic activation of invariant Natural Killer T cells, Front. Immunol. 9 (2018).
[20] L. Van Kaer, L. Wu, Therapeutic potential of invariant natural killer T cells in autoimmunity, Front. Immunol. 9 (2018) 519.
[21] J.L. Matsuda, T. Mallevaey, J. Scott-Browne, et al., CD1d-restricted iNKT cells, the Swiss-Army knife' of the immune system, Curr. Opin. Immunol. 20 (2008) 358.

[22] M. Noto Llana, S.H. Sarnacki, A.L. Morales, et al., Activation of iNKT cells prevents salmonella-enterocolitis and salmonella-induced reactive arthritis by down-regulating IL-17-producing γδT cells, Front. Cell. Infect. Microbiol. 7 (2017) 398.
[23] J. Guillaume, N. Pauwels, S. Aspeslagh, et al., Synthesis of C-5″ and C-6″-modified α-GalCer analogues as iNKT-cell agonists, Bioorg. Med. Chem. 23 (13) (2015) 3175–3182.
[24] S. Mansour, A.S. Tocheva, J.P. Sanderson, et al., Structure and functional change of the iNKT clonal repertoire in early rheumatoid arthritis, J. Immunol. 195 (12) (2015) 5582–5591.
[25] P.J. Brennan, M. Brigl, M.B. Brenner, Invariant natural killer T cells: an innate activation scheme linked to divers, Nat. Rev. Immunol. 13 (2) (2013) 101–117.
[26] Y. Koguchi, A.C. Buenafe, T.J. Thauland, et al., Preformed CD40L is stored in Th1, Th2, Th17, and T follicular helper cells as well as CD4+ 8− thymocytes and invariant NKT cells but not in Treg cells, PLoS One 7 (2) (2012) e31296.
[27] K.M. Walker, M. Rytelewski, D.M. Mazzuca, et al., Preventing and curing citrulline-induced autoimmune arthritis in a humanized mouse model using a Th2-polarizing iNKT cell agonist, Immunol. Cell Biol. 90 (6) (2012 Jul) 630–639.
[28] K. Coppieters, K. Van Beneden, P. Jacques, et al., A single early activation of invariant NK T cells confers long-term protection against collagen-induced arthritis in a ligand-specific manner, J. Immunol. 179 (2007) 2300–2309.
[29] Masanobu Horikoshi, Daisuke Goto, Seiji Segawa, et al., Activation of invariant NKT cells with glycolipid liganda-galactosylceramide ameliorates Glucose-6-phosphate isomerase peptide-induced arthritis, PLoS One 7 (12) (2012) e51215.
[30] A. Chiba, S. Oki, K. Miyamoto, H. Hashimoto, T. Yamamura, S. Miyake, Suppression of collagen-induced arthritis by natural killer activation with OCH, a sphingosine-truncated analog of a-galactosylceramide, Arthritis Rheum. 50 (2004) 305–313.
[31] Susan J. Tudhope, Alexei von Delwig, Jane Falconer, et al., Profound invariant natural killer T-cell deficiency in inflammatory arthritis, Ann. Rheum. Dis. 69 (2010) 1873–1879.
[32] Loes Linsen, Marielle Thewissen, Kurt Baeten, et al., Peripheral blood but not synovial fluid natural killer T cells are biased towards a Th1-like phenotype in rheumatoid arthritis, Arthritis Res. Ther. 7 (2005) R493–R502.
[33] Adam K. Savage, Michael G. Constantinides, Jin Han, et al., The transcription factor PLZF (Zbtb16) directs the effector program of the NKT cell lineage, Immunity 29 (3) (2008) 391–403.
[34] A.P. Mao, I.E. Ishizuka, D.N. Kasal, et al., A shared Runx1-bound Zbtb16 enhancer directs innate and innate-like lymphoid lineage development, Nat. Commun. 8 (1) (2017) 863.
[35] A.J. White, B. Lucas, W.E. Jenkinson, et al., Invariant NKT cells and control of the *Thymus medulla*, J. Immunol. 200 (10) (2018) 3333–3339.
[36] L. Lynch, X. Michelet, S. Zhang, et al., Regulatory iNKT cells lack PLZF expression and control Treg cell and macrophage homeostasis in adipose tissue, Nat. Immunol. 16 (1) (2015) 85.
[37] Y. Jin, H.Z. Nenseth, F. Saatcioglu, Role of PLZF as a tumor suppressor in prostate cancer, Oncotarget 8 (41) (2017) 71317.